We are IntechOpen,
the world's leading publisher of
Open Access books
Built by scientists, for scientists

4,800
Open access books available

122,000
International authors and editors

135M
Downloads

Our authors are among the

154
Countries delivered to

TOP 1%
most cited scientists

12.2%
Contributors from top 500 universities

BOOK CITATION INDEX

CLARIVATE ANALYTICS

INDEXED

WEB OF SCIENCE™

Selection of our books indexed in the Book Citation Index
in Web of Science™ Core Collection (BKCI)

Interested in publishing with us?
Contact book.department@intechopen.com

Numbers displayed above are based on latest data collected.
For more information visit www.intechopen.com

Co-Channel Interference Cancellation for 5G Cellular Networks Deploying Radio-over-Fiber and Massive MIMO Beamforming

Sheng Xu

Abstract

In future fifth-generation (5G) wireless cellular networks, distributed massive multiple-input multiple-output (MIMO) techniques will be applied worldwide. Recently, much more challenges on efficient resource allocation to large numbers of user equipment (UE) are raised in order to support their high mobility among different micro-/pico-cells. In this chapter, we propose a framework to enable an optical back-haul cooperation among different optical network units (ONUs) with distributed MIMO techniques in wireless front-haul for next-generation optical-wireless cellular networks. Specifically, our proposal is featured by a downlink resource multi-cell sharing scheme for OFDMA-based passive optical network (PON) supporting radio-over-fiber (RoF). We first consider system architecture with the investigation of related works, and then we propose a co-channel interference mitigation and delay-aware sharing scheme for real-time services allowing each subcarrier to be multi-cell shared by different active ONUs corresponding to different micro-/pico-cells. Furthermore, a heuristic algorithm to mitigate co-channel interference, maximize sharing capacity, and minimize network latency is given by employing the graph theory to solve such sharing problems for future 5G. Finally, simulations are performed to evaluate our proposal.

Keywords: co-channel interference, 5G, distributed MIMO, passive optical networks, OFDMA, radio-over-fiber

1. Introduction

The increasing demand of real-time services (e.g., VoIP, the video telephony, and streaming) poses high requirements on communication quality (e.g., interference mitigation and delay constraint) and bandwidth increase in the network for the future era of big data [1]. Nowadays, the OFDMA-based passive optical network (PON) has been applied to provide such a large-capacity and also high-flexibility solution for wireless cellular networks with radio-over-fiber (RoF) technology [2, 3].

Figure 1 describes a RoF-based optical-wireless system adopting OFDMA-PON, while one of prominent challenges in such networks for future 5G communications is the algorithm for effective resource allocation. In the related works, a dynamic bandwidth allocation (DBA) in OFDMA-PON has been implemented in [4] with fixed subcarriers for data scheduling, which adopts a traditional grant/report polling scheme. Moreover, dedicated resource allocation (DRA) and shared resource allocation (SRA) as two DBA methods were proposed in [5]. The DBA protocol in OFDM-PON therefore has been proposed in [6], where protocols are summarized in two schemes: the fixed burst transmission (FBT) and the dynamic circuit transmission (DCT). FBT employs a round-robin, IPACT algorithm [6] while DCT adopts bandwidth estimation. Furthermore, a power-efficient DBA scheme of OFDM-PON has also been given in [7] for the purpose of minimizing the optical network units (ONUs) transmitting power. In addition, a lot of works such as for attaining the low power consumption with OFDM-PON have been finished on a system hardware level. Specifically, a 36.86-Gb/s optical wavelength conveying six 100-MHz-bandwidth LTE-A signals has been proposed in [8]. The system supports 5-carrier aggregation, 2×2 MIMO, and three sectors, over a 40-km SSMF front-haul adopting a single 1550-nm directly modulated laser. In addition, the system [2] adopts a fixed RF channel on subcarriers; however, it becomes inflexible to satisfy DBA when high mobility of large number of user equipment (UE) occurs in the wireless front-haul. The structure [2, 3] deploys an optical distribution network (ODN), which is different with [4, 5], but the DBA problem is still the same.

However, considering a very high density level of UEs and their high mobility in future 5G cellular networks, a prominent problem waiting to be solved is the co-channel interference jointly employing radio-over-fiber, massive multiple-input and multiple-output (MIMO), and beam-forming [9] technologies. For example, in optical-wireless networks, when the same wireless frequency resources carried by different optical wavelengths overlap in the same beam direction
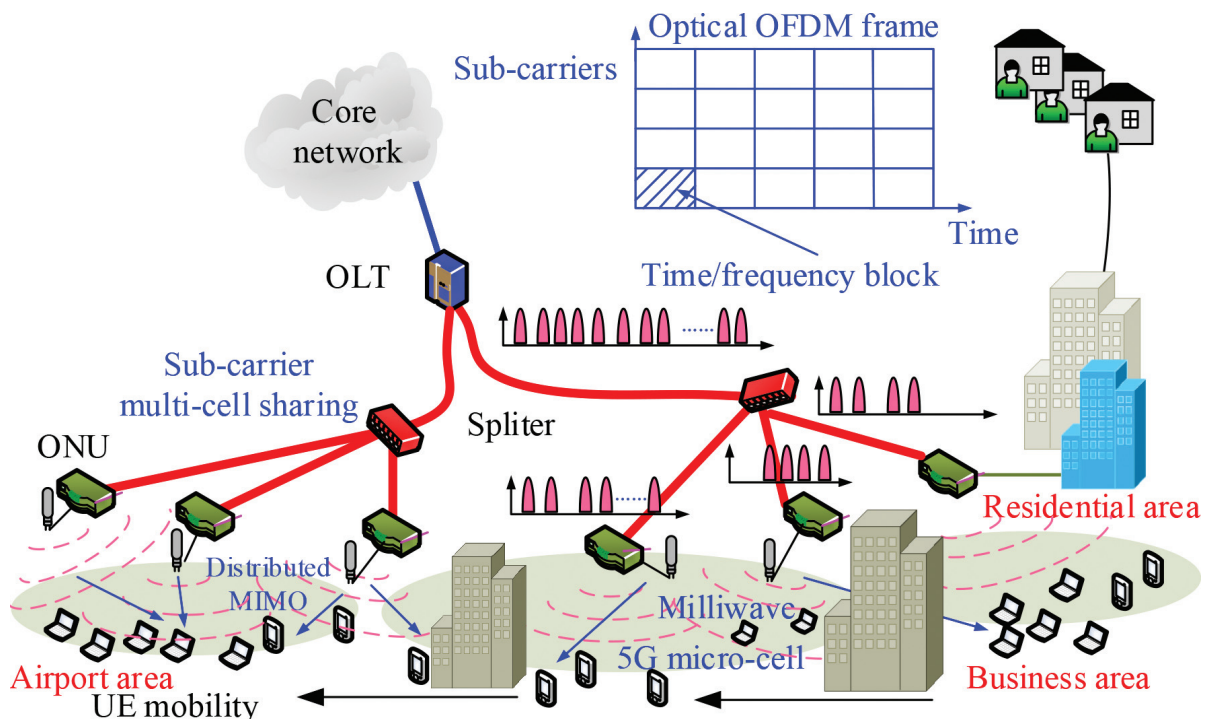

Figure 1. Network architecture of RoF-OFDM-PON based on 5G [9].

and are received by different UEs, these UEs which emerge in this beam direction under their mobility will suffer high interference. Typically, in the case of distributed massive MIMO, numbers of UEs move frequently among a few of micro-/pico-cells in any time; wireless data carried over the wavelength are shared by all served UEs in the pico-cell and adjacent cells. The minimizing of co-channel interference as mentioned will become much more imperative. Hence, it is expected to seek a scheduling optimization of wireless resources to each micro-cell mitigating the interference due to high UE mobility. Furthermore, we consider a given limited number of optical subcarriers, when an ONU needs additional resources, and in order to support the bandwidth demand for the rest of ONUs, optical subcarriers will not be reallocated in congestion cases, the problem herein is also to find ways to share optical subcarriers among local different cells by ONUs. However, it brings the additional delay problem and also configuration and control problem for selecting ONUs because of resource sharing and transmission. To achieve these targets, we propose and observe an interference mitigation and delay-aware sharing scheme for real-time services allowing that each subcarrier of RoF-OFDM-PON [2] can be multi-cell shared by UEs accessed from different micro-cells. Namely, each UE is arranged to receive multiple data streams demodulated from different ONUs simultaneously.

In this chapter, we address the aforementioned problems in the system, which have not been studied in other works before. The proposed method in this chapter can be employed by a future 5G operator to run radio-over-fiber based optical OFDM (OOFDM) [3] networks with multiple micro-/pico-cells as shown in **Figure 1**; it could be used as a method on network design to reduce resource waste and improve the performance of network.

The rest of this chapter is organized as follows. Section 2 presents our system architecture and resource allocation model. Section 3 introduces our resource sharing proposal. A heuristic algorithm guaranteeing minimum co-channel interference, maximum sharing capacity, and minimum delay time is presented in Section 4. Section 5 provides evaluation results with simulations. Finally, the chapter is concluded in Section 6.

2. RoF-OFDM-PON system

2.1. Link architecture in RoF-OFDM-PON networks

Figure 2 illustrates an experimental link architecture for signal processing in RoF-OFDM-PON [10] to support our proposal and to be employed as a physical infrastructure for one data stream in system. From the transmitter side, this implementation firstly modulates experimental data through an OFDM processing with performing of the PRBS, NRZ pulse, and QAM sequence generation (e.g., 4-QAM) in advance [10]. After that, a RF-IQ mixer is used to deal with the OFDM signal to analog RF with a proper quadrature modulation. The output signal then experiences an optical OFDM (OOFDM) modulation with a 193.1 THz CW laser by LiNbO3 mach-zehnder modulator (MZM) [10, 11] and then is sent into fiber through EDFA to amplify the signal.

On each receiver of ONU side, signals from fiber are received by photo-detector (PD) [10, 11] and are executed with a RF de-multiplexing and OFDM demodulation followed by QAM sequence generator and NRZ pulse generator in order to recovery the experimental data [10]. It is important to note that one set of optical OFDM subcarrier on fiber could be modulated to
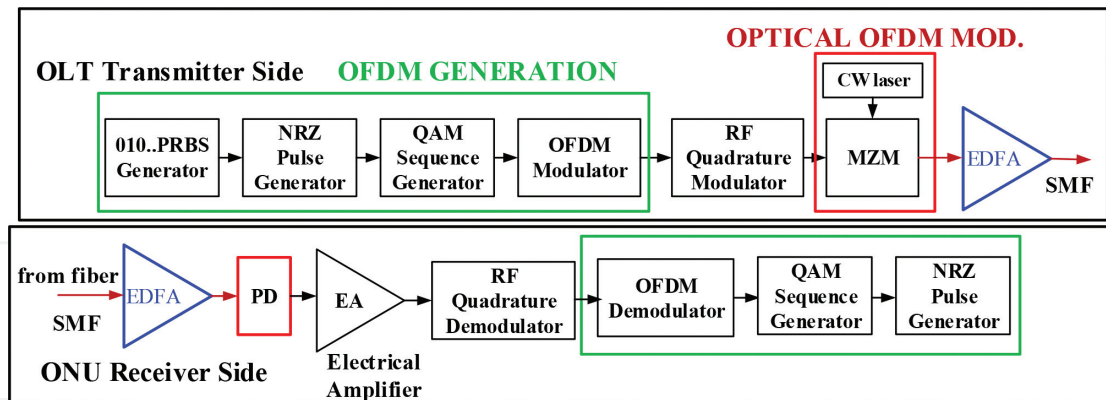
Figure 2. The downlink signal processing of RoF-OFDM-PON.

accommodate different UEs belonging to two or more receivers/ONUs in cellular networks, and the wireless data allocated to UEs belonging to any micro-cell could be transmitted by the broadcasting of multiple sharing streams from other ONUs with antennas in other micro-cells nearby (e.g., by the distributed massive MIMO [9]). In this chapter, our work thus mainly consider these resource allocation problems, while detailed physical discussions on the control and configuration issues (e.g., protocol specification) for dynamic transmission from multiple ONUs for resource sharing are out of the scope of this chapter.

2.2. Optical subcarrier allocation model

Employing the downlink signal processing mentioned in Section 2, the current OFDM-PON access networks flexibly allocate the time/frequency blocks in OFDM frame logically as shown in **Figure 3** under a mixed access rate. **Figure 3** describes an example about resource allocation of optical time/frequency block distributed to three different ONUs under different time slots and optical subcarriers. In this case, multiple wireless UE data are modulated onto each time/frequency block, and each block could be allocated to a single ONU, while each ONU could receive several such time/frequency blocks in the same time slot [12, 13]. Each optical subcarrier of time/frequency block in **Figure 3** could be addressed by a RoF modulation with radio frequency in the same or different wireless radio frequency spectra (e.g., a LTE radio frame frequency spectrum from 2110 to 2170 MHz) [14]. Moreover, according to the bandwidth capacity of single optical carrier, multiple radio frame could be conveyed on a single carrier (e.g., as reported in [8], six 100 MHz LTE-A signals are conveyed on a 36.86 Gb/s optical carrier).

Adopting this subcarrier allocation method, different UEs are fed by its ONU within its cell, and the subcarrier number allocating to each ONU could be appended according to the increase of traffic in this cell. However, the very high UE mobility in future 5G pico-cells [9] results that a few idle resource appears on a signal optical time/frequency block so that much more wasted resource is produced during resource allocation. In order to rationally allocate these idle resources (e.g., the remnant resource in **Figure 4** during slot t_2), it should be noted that the physical optical modulation process in **Figure 2** can be easily controlled to make UE data belonging to different ONUs be modulated onto the same optical time/frequency block with radio-over-fiber, as shown in **Figure 4**. For instance, in **Figure 4**, ONU 3 has idle resources in time slot t_1; however, its data requirement exceeds the allocated amount from time slot t_3 on.
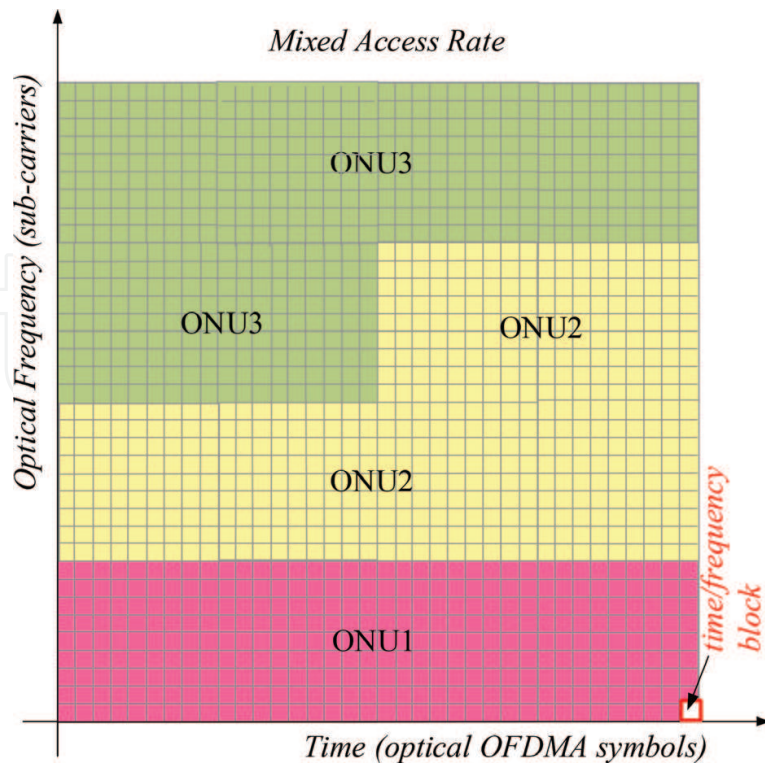
Figure 3. Optical OFDMA frame with time/frequency block allocation to different ONUs in RoF-OFDM-PON systems [12].
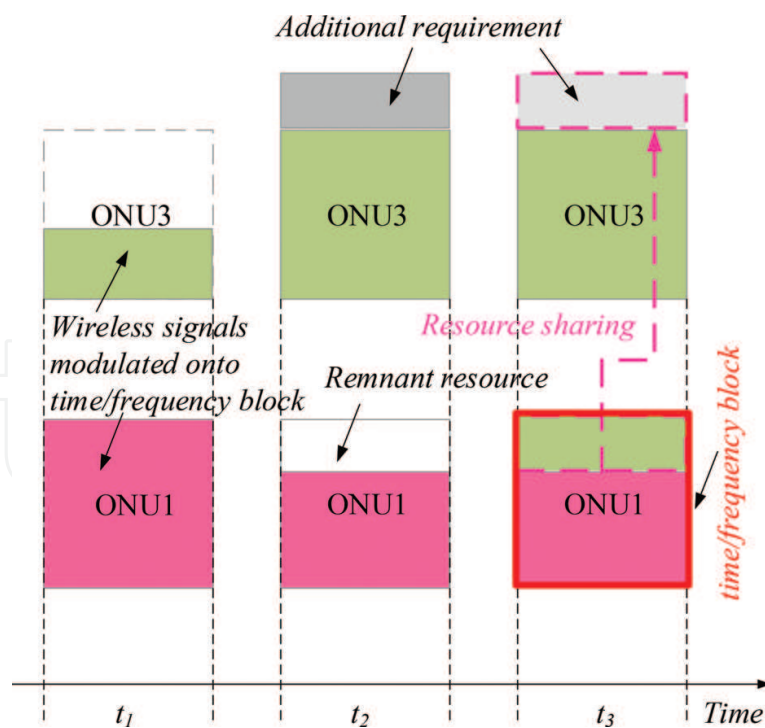

Figure 4. Multi-cell sharing of wireless resources on optical time/frequency blocks allocated to different ONUs corresponding to different wireless cells.

With our proposal, it will receive remnant resources of ONU 1 in time slot t_3 by real-time resource sharing for its additional requirement.
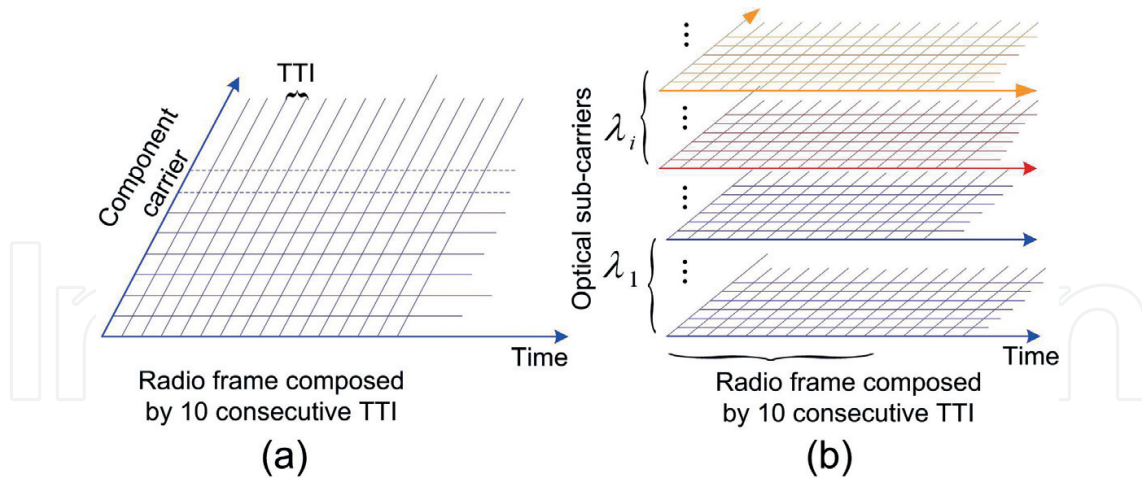
Figure 5. Wireless resource sharing logically on optical time/frequency blocks by different ONUs.

2.3. Radio frame model on optical subcarriers

The wireless spectrum resource can be illustrated by **Figure 5(a)**. In contrast to the single-layer radio frame which is illustrated in **Figure 5(a)**, by allocating more subcarriers, multiple radio frames can be delivered on fiber to each ONU, forming the multi-layer radio frames which are shown in **Figure 5(b)** for each ONU. Note that **Figure 5(b)** describes multiple wireless frames carried by a single optical subcarrier λ_i. Therefore, the time slot in **Figure 5** is different from that in **Figures 3** and **4**, for example, optical scheduling time slot t_1 in **Figure 4** contains several consecutive time slots in **Figure 5** which is named as transmission time interval (TTI) [15].

Note that the smallest optical resource unit in **Figures 3** and **4** is named as time/frequency block, while the smallest radio resource unit in **Figure 5** is named as resource block (RB). They are different concepts in this chapter. Each component carrier (CC) contains several RBs [14, 15]. One UE can receive several CCs in a certain time slot simultaneously.

3. Mathematical optimization

3.1. Assumptions of the model

Assumption 1: There are total $N^i_{\text{sub-c}}$ optical subcarriers allocated to ONU i, and l is the indicator of optical subcarrier. For each l-th optical subcarrier, it contains C_l layers of frames, as shown in **Figure 6(b)**. p is the indicator of frame on each optical subcarrier. The concept of multi-layer frames will be adopted in the following problem description and resource sharing algorithm.

Assumption 2: Denote $R_{k,t}$ as the minimum capacity requirement for user k in slot t. The UE set $\{1, 2, \ldots, \tilde{k}, \ldots, \tilde{K}\}$ is served by ONU i, while UE set $\{1, 2, \ldots, k, \ldots, K\}$ is served by ONU j. Denote $N_{\text{sub-c}}$ as the consecutive subcarrier number on frequency of each RB and N_{sym} as OFDM symbol [14] number on time domain of each RB. In addition, denote $N_{\text{sc}}^{(d)}{}_s$ as the subcarrier number for date transmission in the s-th OFDM symbol, and $N_{\text{sc}}^{(d)}{}_s < N_{\text{sub-c}}$, because of the existence of subcarriers used for control signals in each RB.
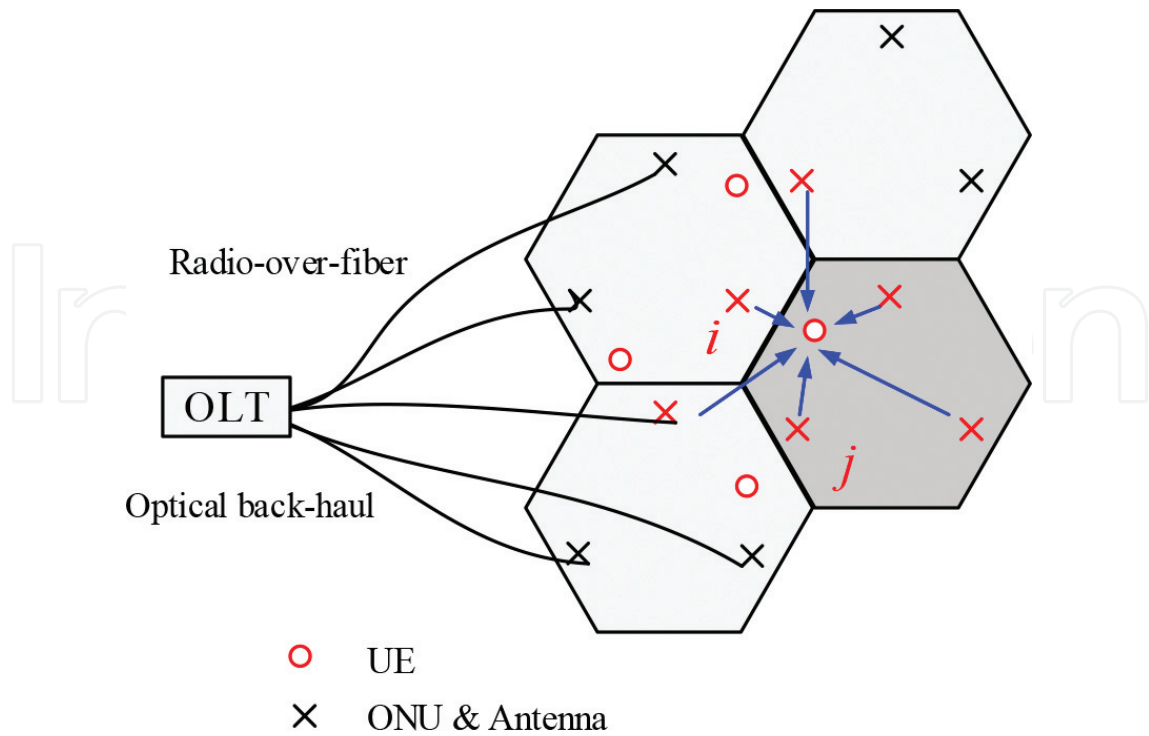
Figure 6. The illustration of multi-cell RoF-OFDM-PON scenarios with distributed massive MIMO deployment. (Each cross represents an ONU/antenna location, while the red circle represents the UE. Six red crosses in different cells highlight that one UE receives multiple data streams in the subcarrier sharing scenario).

Assumption 3: There are J numbers of modulation and coding scheme (MCS) for each RB to choose, and $R_o^{(c)}$ is code rate in a dedicated MCS, $o \in \{1, 2,...., J\}$. M_o describes the constellation size of MCS [14]. In each TTI of scheduling, the capacity $r^{(o)}{}_{\mathrm{RB}}$ for one RB under MCS o is then given by Eq. (1):

$$r_{\mathrm{RB}}^{(o)} = R_o^{(c)} \log_2(M_o) \sum_{s=1}^{N_{\mathrm{sym}}} N_{\mathrm{sc}\ s}^{(d)}$$

(1)

Assumption 4: Suppose that $g_{k,l,p,n}$ indicates the wireless channel quality indicator (CQI) [14] of the n-th RB in each CC carried on the p-th optical subcarrier dedicated to UE k. The CQI of RB in each CC carried on the p-th frame on l-th optical subcarrier can be given by $g_{k,l,p} = [g_{k,l,p,1}, g_{k,l,p,2},..., g_{k,l,p,N_{\mathrm{RB}}}]^{\mathrm{T}}$. Each UE can employ at most z CCs to receive data in each slot. Each UE can only adopt one MCS for its assigned RB of CCs.

Assumption 5: We consider beam-forming [7] for wireless signal propagation. In terms of beam direction of the i-th ONU/antenna pair, two categories of UEs' conflict relationship according to any two UEs' locations (from the view point of the i-th ONU/antenna pair) are (1) same angle UEs and (2) different angle UEs. Define a matrix $\chi_i = [\chi_i(1, 2),..., \chi_i(k, k'),..., \chi_i(K-1, K)]$. The value of $\chi_i(k, k')$ is then defined in the Eq. (2).

$$\chi_i(k, k') = \begin{cases} 0; \text{different angle UEs} \\ 1; \text{the same angle UEs} \end{cases}$$

(2)

Naturally, different beam directions can mitigate interference. For any two UEs, from a view point of the ONU/antenna pair, the first category (i.e., $c_i(k, k') = 1$) is that two UEs locate at the same angle of beam direction. The second category (i.e., $c_i(k, k') = 0$) is that two UEs locate at different beam directions. Hence, the co-channel interference of second category UEs will be mitigated, even if these UEs employ the same RB of CCs on different radio frames which are carried by different optical subcarriers. However, for the first category UEs, interference still occurs if the UEs employ the same RB of CCs on different radio frames.

Therefore, $\gamma^{(n,y,t)}_{k, k'}$ is also defined as a binary variable. As shown in Eq. (3), $\gamma^{(n,y,t)}_{k, k'} = 1$ indicates that the same RB n of the y-th CC is allocated to UE k and k' in slot t at different frames. The same RB of CCs here means the RB on component carriers in the same frequency and also the same time slot carried by different frames:

$$\gamma^{(n,y,t)}_{k, k'} = \begin{cases} 1; & \text{UE } k \text{ and } k' \text{ are allocated with the same RB of CC} \\ 0; & \text{otherwise} \end{cases} \tag{3}$$

Definition 1: The UE set $\{1, 2,\ldots, \tilde{k},\ldots, \tilde{K}\}$ is located outside the cell ξ and served by ONU i, while UE set $\{1, 2,\ldots, k,\ldots, K\}$ is in the cell ξ and served by ONU j.

Definition 2: For any two UEs, from the viewpoint of the MIMO antenna, we define that the same angle UEs in Eq. (2) are two UEs located at the same angle of beam direction. The angle space depends on the coverage of a beam released by antennas (e.g., 30° or the case of narrow beam in 5G). Otherwise, they are different angle UEs which locate at different beam directions (base station MIMO antenna arrays in the cell are in the same place and treated as one point).

3.2. Modeling of resource sharing proposal

The optimization model we proposed is more applicable for the deployment of small cell coverage with a high UE mobility scenario, so that the sharing capacity can be maximized and the delay time from the OLT to each UE could be minimized by the model. In the system, we suppose a remnant resource of bandwidth of each ONU after its inter-cell allocation can be delivered to the UEs in different cells for resource sharing by the broadcasting of distributed antennas. It is assumed that the antenna transmission for wireless signals in each cell could well reach the UEs in several adjacent cells. We also suppose that each ONU is attached by one antenna element in its location by default. In this chapter, for simplicity, we directly denote i or j as an ONU/antenna pair, that is, the ONU i means the ONU in i-th ONU/antenna pair, and the ONU j means the ONU in j-th ONU/antenna pair. Especially, in terms of UE k which located in cell ξ, we define ONU i for the ONU placed outside cell ξ and ONU j for the ONU placed in cell ξ. The UE set $\{1, 2,\ldots, \tilde{k},\ldots, \tilde{K}\}$ is located outside the cell ξ and served by ONU i, while UE set $\{1, 2,\ldots, k,\ldots, K\}$ is in the cell ξ and served by ONU j. The classification of different UE sets and different ONU/antenna pairs is to clearly describe the optimization problem of subcarrier multi-cell sharing.

Consider the single UE k which is accommodated by ONU j, and UE k receives data from ONU j and a shared ONU i. For the data stream from ONU i to UE k, we define $d^k_{i,t}$ as its delay of sharing data for UE k in time slot t by ONU i from optical back-haul in OLT to the UE.

We consider the case that multiple ONUs share their data for a single UE k. As the system model depicted in **Figure 6**, we define a set $\mathcal{M} = \{i \mid i = 1, 2,\ldots, b,\ldots, m\}$ which represents the set of ONUs outside the cell where UE k is located for bandwidth sharing to UE k.

On the other hand, we define $\mathcal{P} = \{j \mid j = 1, 2,\ldots, b,\ldots, n\}$ representing the set of ONUs inside the cell where UE k belongs and $\mathcal{N} = \{i \mid i = 1, 2,\ldots, b,\ldots, n\}$ representing the set of total ONUs in a local network, respectively. Here, m is less than n and $\mathcal{M} \cup \mathcal{P} \subseteq \mathcal{N}$. For the parameter b, note that the delay time $d^k_{b,t}$ is the maximum delay in sharing links among all the links through the selected ONUs to the UE k satisfying:

$$b = \arg \max_{i \in \mathcal{M}} d^k_{i,t} \tag{4}$$

We could enrich our model to the real-time scenario for multiple UEs. The joint objective to (i) maximize sharing capacity with minimum delay and (ii) to minimize co-channel interference in a time duration T can be formulated by Eq. (5) in detail.

Objective:

$$\max\left\{\sum_{t=1}^{T}\sum_{k=1}^{K}\left(\sum_{i=1, i\neq j}^{m} w^k_{i,t} \cdot c^k_{i,t} - \sum_{i=1, i\neq j}^{m} q^k_{i,t} \cdot d^k_{i,t}\right) - \sum_{i=1, i\neq j}^{m}\sum_{t=1}^{T}\sum_{y=1}^{N_{CC}}\sum_{n=1}^{N_{RB}}\left(\sum_{C_i(k,k')=1} \gamma^{(n,y,t)}_{k,k'} + \sum_{C_i(k,\bar{k})=1} \gamma^{(n,y,t)}_{k,\bar{k}}\right)\right\} \tag{5}$$

where $w^k_{i,t}$ and $q^k_{i,t}$ can be further described in Eqs. (6) and (7), respectively:

$$w^k_{i,t} = \beta^k_{i,t} \cdot G^k_{i,t} \cdot \min\left\{h^k_{i,t-1}, h^k_{i,t-2}, \ldots, h^k_{i,1}\right\} \tag{6}$$

$$q^k_{i,t} = \beta^k_{i,t} \cdot D^k_{i,t} \cdot \max\left\{U^k_{i,t-1}, U^k_{i,t-2}, \ldots, U^k_{i,1}\right\} \tag{7}$$

Here, $\beta^k_{j,t}$ represents a binary indicator that UE k is served or not by ONU i in slot t. Different from $c^k_{i,t}$ which is a current capacity that could be provided to UE k in slot t, while $G^k_{i,t}$ is a current capacity which is obtained by UE k finally in slot t. Moreover, $h^k_{i,t-1}$ is a historical capacity obtained by UE k in slot t-1. It should be noted that $c^k_{i,t}$ is the shared capacity available for UE k from ONU i. Meanwhile, in Eq. (7), $D^k_{i,t}$ and $U^k_{i,t-1}$ are current delay constraint of UE k in slot t and historical delay record of UE k in slot t-1, respectively.

The optimization objective in Eq. (5) may be seemed indeed as an interference mitigation problem of finding $c^k_{i,t}$ subjected to the delay requirement from a set of $\mathcal{M} = \{i \mid i = 1, 2,\ldots, b,\ldots, m\}$ for UE k severed by ONU j. This will be solved in more details in our heuristic algorithms later. Firstly, we discuss all the constraints of objective as follows;

1) Capacity constraints for UE k:

$$\sum_{i \in \mathcal{M}, i\neq j} c^k_{i,t} \geq A^k_t - \sum_{j \in \mathcal{P}} F^k_{j,t} \tag{8}$$

Equation (8) describes the total sharing capacity should not be less than the capacity requirement for each UE k in each time slot t. A^k_t is total data capacity demand of UE k and $F^k_{j,t}$ is data capacity provided by ONU j to UE k.

2) Delay constraints for UE k:

$$d_{b,t}^k \leq D_{i,t}^k \tag{9}$$

The delay constraint in Eq. (9) in each slot t means that the delay time spent on the path from the source of OLT to the destination of UE should not exceed the maximum tolerable transmission delay time (TDT) of UE k in a real-time service.

3) Capacity constraint for ONU i

Considering the 5G communication with carrier aggregation from [14, 16], we may further discuss the constraint of $c_{i,t}^k$:

$$\sum_{k=1}^{K} c_{i,t}^k \leq E_{i,t} \tag{10}$$

Denote $E_{i,t}$ as the total remaining capacity of ONU i after the allocation for its UEs accommodated. Equation (10) describes that the total amount of sharing capacity of UEs should be less than $E_{i,t}$.

With respect to our resource allocation model for optical time/frequency blocks with RoF and downlink signal processing in Section 2, we formulate $E_{i,t}$ approximately with the aforementioned assumptions which are detailed in the aspect on resource allocation.

The remaining capacity $E_{i,t}$ of ONU i in time slot t is then given as Eq. (11) approximately:

$$E_{i,t} = \sum_{l=1}^{N_{\text{sub-c}}^i} C_l \left(\frac{1}{Q} N_{\text{cc}} N_{\text{RB}} \sum_{o=1}^{Q} r_{\text{RB}}^{(o)} \right) - \sum_{l=1}^{N_{\text{sub-c}}^i} \sum_{p=1}^{C_l} \sum_{\tilde{k}=1}^{\tilde{K}} \sum_{y=1}^{N_{\text{cc}}} \sum_{n=1}^{N_{\text{RB}}} \sigma_{\tilde{k},l,p}^{(n,y,t)} \sum_{o=1}^{Q} \mu_{\tilde{k},o} \cdot r_{\text{RB}}^{(o)} \tag{11}$$

Especially, $\sigma_{k,l,p}^{(n,y,t)}$ is a binary variable to define whether or not the n-th RB of the y-th CC is assigned to the k-th UE on the p-th frame on the l-th optical sub-carrier in slot t, and $\sigma_{k,l,p}^{(n,y,t)} = 1$ expresses that allocating the n-th RB of the y-th CC to the k-th UE in slot t. Here, we define a binary variable $\mu_{k,o} = 1$ to express that the k-th UE employs the o-th MCS. Q in Eq. (13) describes the highest MCS employed by the k-th UE corresponding to a CQI of RB "$max(g_{k,l,p,\delta*})$" in each CC of the p-th frame on the l-th optical subcarrier. Here:

$$\delta^* = \underset{n \in \{1,2,\dots,N_{\text{RB}}\}}{\arg\max} \left(g_{k,l,p,n} \right) \tag{12}$$

$$Q_{k,l,p,\max(g_{k,p,\delta*})} = \underset{j \in \{1,2,\dots,J\}}{\text{argmax}} \left(R_j^{(c)} \log_2(M_j) \Big| g_{k,l,p,\delta*} \right) \tag{13}$$

In the Eq. (11), $N_{\text{sub-c}}^i$, N_{cc}, and N_{RB} are the number of optical subcarriers allocated to ONU i by OFDM-PON, the total number of wireless component carriers (CC) [15, 16] modulated onto a single optical subcarrier, and total number of wireless resource blocks (RB) carried by a single wireless component carrier (CC), respectively. The second term of polynomial in Eq. (11)

should be larger than the summation of total UE minimum capacity requirement. Hence, a constraint of $c^k_{i,t}$ can be further formulated as in Eq. (14),

$$\sum_{k=1}^{K} c^k_{i,t} \le E_{i,t} \le \sum_{l=1}^{N^i_{sub-c}} C_l \left(\frac{1}{Q} N_{cc} N_{RB} \sum_{o=1}^{Q} r^{(o)}_{RB} \right) - \sum_{\tilde{k}=1}^{\tilde{K}} R_{\tilde{k}} \tag{14}$$

In the following allocation algorithm, we will satisfy all the aforementioned constraints to find the sharing capacity $c^k_{i,t}$ for UE k from ONU i.

4) Interference constraint for UEs

In terms of the i-th ONU/antenna pair, the constraint of $\gamma^{(n,y,t)}_{k,\tilde{k}}$ is described in Eq. (15). It means that the number of same RB of CC allocated to different UEs on all the frames carried by optical subcarriers has an upper limitation. Since $\gamma^{(n,y,t)}_{k,\tilde{k}}$ is a binary indicator, Eq. (15) could be treated as two cases. First, when $\gamma^{(n,y,t)}_{k,\tilde{k}} = 1$, the same RB n of the y-th CC is allocated to UE k and $\tilde{k}$ in slot t at different frames, the product of all the numbers of these RBs allocated to UE k and all the number of same RBs allocated to UE $\tilde{k}$ must not be larger than their arithmetic mean square, while the upper limitation of their arithmetic mean equals half of the number of total frames. Second, when $\gamma^{(n,y,t)}_{k,\tilde{k}} = 0$, any RB n of the y-th CC is not allocated to both UE k and $\tilde{k}$ in slot t at different frames; therefore, for all the number of RBs allocated to UE k and $\tilde{k}$, their product must equal to 0 (i.e., without RB overlapping on the same time/frequency domain) as described in Eq. (15):

$$\sum_{l=1}^{N^i_{Sub-c}} \sum_{p=1}^{C_l} \sigma^{(n,y,t)}_{k,l,p} \cdot \sum_{l=1}^{N^i_{Sub-c}} \sum_{p=1}^{C_l} \sigma^{(n,y,t)}_{\tilde{k},l,p} \le \gamma^{(n,y,t)}_{k,\tilde{k}} \left[\frac{1}{2} \left(\sum_{l=1}^{N^i_{Sub-c}} \sum_{p=1}^{C_l} \sigma^{(n,y,t)}_{k,l,p} + \sum_{l=1}^{N^i_{Sub-c}} \sum_{p=1}^{C_l} \sigma^{(n,y,t)}_{\tilde{k},l,p} \right) \right]^2 \le \gamma^{(n,y,t)}_{k,\tilde{k}} \left[\frac{1}{2} \left(\sum_{l=1}^{N^i_{Sub-c}} C_l \right) \right]^2, \tag{15}$$

$$\forall k, \tilde{k}, \forall y, \forall n, \forall t$$

Similarly, we hereby obtain the following constraint of $\gamma^{(n,y,t)}_{k,k'}$ as described in Eq. (16):

$$\sum_{l=1}^{N^i_{Sub-c}} \sum_{p=1}^{C_l} \sigma^{(n,y,t)}_{k,l,p} \cdot \sum_{l=1}^{N^i_{Sub-c}} \sum_{p=1}^{C_l} \sigma^{(n,y,t)}_{k',l,p} \le \gamma^{(n,y,t)}_{k,k'} \left[\frac{1}{2} \left(\sum_{l=1}^{N^i_{Sub-c}} \sum_{p=1}^{C_l} \sigma^{(n,y,t)}_{k,l,p} + \sum_{l=1}^{N^i_{Sub-c}} \sum_{p=1}^{C_l} \sigma^{(n,y,t)}_{k',l,p} \right) \right]^2 \le \gamma^{(n,y,t)}_{k,k'} \left[\frac{1}{2} \left(\sum_{l=1}^{N^i_{Sub-c}} C_l \right) \right]^2, \tag{16}$$

$$\forall k, k', \forall y, \forall n, \forall t$$

4. Proposed resource sharing algorithm

In this section, we propose a heuristic algorithm for obtaining sub-optimal solutions because solving the objective in Section 3 is highly complex. A natural and simple approach to address the joint objectives of Eq. (5) is to treat it as a maximum flow and minimum cost problem about resource allocation (e.g., RB of CC) by assigning $\sigma^{(n,y,t)}_{k,l,p}$ we defined for UE in each slot, approximately. We record and observe some historical information (e.g., $h^k_{j,t-1}$ and $U^k_{j,t-1}$) as timely references and evaluations for finding a maximum flow ($c^k_{i,t}$) subjected to the delay requirement ($d^k_{i,t}$) with minimum delay time from a set of $\mathcal{M} = \{i \mid i = 1, 2, ..., b, ..., m\}$ for UE

k severed by ONU j. In the following sections, the sharing path assignment and the corresponding resource allocation will be detailed in algorithm descriptions by transferring the problem into the optimization with the aid of graph theory.

4.1. Problem statement

- *Given parameters*:

    - $G\,(\mathcal{V},\,\mathcal{E})$ where $\mathcal{V}$ is UE k and set of all ONUs and $\mathcal{E}$ is the set of resource sharing path through multiple ONUs to UE k

    - Matrix $C_{k,t} = [c^k_{1,t},\ldots,\,c^k_{i,t},\ldots,\,c^k_{N,t}],\,\forall\,k$ in $\mathcal{K}$, $c^k_{i,t} > 0$

    - Matrix $\mathcal{D}_{k,t} = [d^{\,k}_{1,t},\ldots,\,d^{\,k}_{i,t},\ldots,\,d^{\,k}_{N,t}],\,\forall\,i$ in $\mathcal{N}$, $\forall k$ in $\mathcal{K}$

    - Matrix $X_i = [\chi_i(1,2),\ldots,\,\chi_i(k,k'),\ldots,\,\chi_i(K-1,K)]$

    - Matrix $\mathcal{Y}_i = [Y_i(k,1),\ldots,\,Y_i(k,\tilde{k}),\ldots,\,Y_i(k,\tilde{K})]$

    - Set of UE in the cell: $\mathcal{K} = \{k\,|\,k = 1,\,2,\ldots,\,K\}$

    - Set of UE outside the cell: $\widetilde{\mathcal{K}} = \{\tilde{k}\,|\,\tilde{k} = 1,\,2,\ldots,\,\tilde{K}\}$

    - Set of ONU: $\mathcal{N} = \{i\,|\,i = 1,\,2,\ldots,\,b,\ldots,\,N\}$

    - $R_{k,t}$: Minimum data capacity requirement for UE k

    - $B_{k,t}$: Allocated data capacity to UE k

Note that X_i and $\mathcal{Y}_i$ are two matrices which store UE conflict relationships.

- *Objective*:

    - Minimize the co-channel interference which is generated by sharing data received for the same angle UEs in their located cell and also in their adjacent cells.

    - Maximize the sharing capacity in terms of UEs.

    - Minimize the average delay of sharing data transmission by ONUs to satisfy UE requirements.

4.2. Algorithm description

The sharing algorithm tries to search the idle RBs over each optical subcarrier delivering to each cell and shares them to the UEs in the adjacent cells. From the sharing paths with minimum delay time, the algorithm selects the paths with maximum number of idle RBs for each UE so that it could maximize the sharing capacity for each UE. Consequently, the algorithm as a solution of optimization problem for our resource allocation model is suggested to be executed on the OLT side of optical back-haul. Considering the single UE k ($k = 1,\,2,\ldots,\,K$) which is accommodated by multiple sharing paths from different ONUs, UE k can receive the

data from each sharing ONU i (i = 1, 2,…, N). The algorithm is divided into several steps as shown in **Tables 1**, **2**, and **3**.

In the first step, a dynamic sharing graph is generated, for instance, **Figure 7(a)** illustrates an example of a sharing tree that five ONUs share bandwidth resources to UE k. The rooted vertex represents UE k, and any leaf vertex i represents ONU i, respectively. Each edge represents a sharing path. In the second step, the weights of vertex and edge are assigned. For the data of UE k from ONU i, $d^k_{i,t}$ denotes the overall delay on sharing path through ONU i to UE k in time slot t. $c^k_{i,t}$ denotes the available sharing data capacity for UE k from ONU i in time slot t.

ALGORITHM 1 Real-time Sharing Algorithm (RTSA)
<Note>:**Algorithm 1** contains **FUNCTION 1, 2** and **3**

Input: Matrix $C_{k,t}$ = {$c^k_{i,t}$ | $c^k_{1,t}$,…, $c^k_{i,t}$,…, $c^k_{N,t}$,∀ $c^k_{i,t}$ > 0}
　　　　 Matrix $\mathcal{D}_{k,t}$ = {$d^k_{1,t}$,…, $d^k_{i,t}$,…, $d^k_{N,t}$}
　　　　 Set of UE: $\mathcal{K}$ = {k | k = 1, 2,…, K}
　　　　 Set of ONU: $\mathcal{N}$ = {i | i = 1, 2,…, b,…, N}
Initialization: G_k = Ø for all k = 1, 2,…, K; G_k: total RB set to UE k
While ($B_{k,t} < R_{k,t}$) do
STEP 1: Make a sharing graph G ($\mathcal{V}$, $\mathcal{E}$); $\mathcal{V}$ = {1,…, N}U{k}, $\mathcal{E}$ = {(i, k) | $d^k_{i,t} \leq D_k$}; D_k is a maximum tolerable delay(MTD).
STEP 2: Assign weights to $\mathcal{E}$ by matrix $\mathcal{D}_{k,t}$ and sort the edges in $\mathcal{E}$ according to its weight in graph G ($\mathcal{V}$, $\mathcal{E}$) in an
　　　　 ascending order.
STEP 3: Find an edge (i, k) with minimum $d^k_{i,t}$ in the ascending order of
　　　　 $\mathcal{E}$ as a current link (i, k) for resource sharing.
STEP 4: $B_{k,t} \leftarrow c^k_{i,t}$ by allocating $\sigma^{(n,y,t)}_{k,l,p}$ until $B_{k,t} \geq R_{k,t}$,
　　　　 otherwise, go to **STEP 3**
STEP 5: Traverse all UEs in set $\mathcal{K}$ to allocate resource satisfying,
　　　　 i = argmin $d^k_{i,t}$, $B_{k,t} \leftarrow c^k_{i,t}$, find $c^k_{i,t}$ employing
　　　　 FUNCTION 1: form G_k
End while
STEP 6: Traverse all ONUs in set $\mathcal{N}$ to allocate resources,
　　　　 repeat **STEPS 1–5**.
STEP 7: Record historical information (e.g., $h^k_{j,t}$ and $U^k_{j,t}$) by **FUNCTION 2**
STEP 8: Update matrix $C_{k,t}$ and matrix $\mathcal{D}_{k,t}$.
End
Out put: G_k = {C_k(1), C_k(2), C_k(i),……, C_k(N)}
End
FUNCTION 1: form G_k, for any k; C_k(i): a RB set from ONU i to UE k
Initialize G_k = {C_k(1), C_k(2), C_k(i),….., C_k(N)} = Ø, set $B_{k,t} \leftarrow 0$.
1: Find ONU i for current link(i, k), where i = argmin $d^k_{i,t}$, set $p \leftarrow 1$.
2: Set $l \leftarrow 1$; l is layer (radio frame) indicator.
3: Find the idle RB for any UE by **FUNCTION 3**,
　　 where $\sigma^{(n,y,t)}_{k,l,p}$ = 0,∀k.
4: Allocate a corresponding idle RB to UE k, put RB of $\sigma^{(n,y,t)}_{k,l,p}$ = 0 into set C_k(i),
　　 then for the UE k,$\sigma^{(n,y,t)}_{k,l,p} \leftarrow 1$. Increase capacity $B_{k,t}$, where, $B_{k,t} = B_{k,t} + r^{(n,y,t)}_{RB k,l,p}$.
5: If $B_{k,t} \geq R_{k,t}$, **break**; $r^{(n,y,t)}_{RB\ k,l,p}$ is the capacity of RB.
　　 Else if ∀k,∀$\sigma^{(n,y,t)}_{k,l,p}$ = 1, i.e., the set of RBs on current layer have been occupied and cannot be scheduled to UE k for
　　　　 sharing, and **if** $l \leq L$ add l, go to **STEP 3**.
　　 Else if $p \leq P_{max-sub}$, add p, go to **STEP 2**.
　　 Else go to **STEP 1**.
　　 End IF
6: Output G_k = {C_k(1), C_k(2), C_k(i),……, C_k(N)}

Table 1. Real-time sharing algorithm.

FUNCTION 2 Historical State Recording

1: Set $h^k_{i,t} = \sum\limits_{p=1}^{N^i_{sub-c}} \sum\limits_{y=1}^{N_{cc}} \sum\limits_{n=1}^{N_{RB}} \sigma^{(n,y,t)}_{k,p} \sum\limits_{o=1}^{Q} \mu_{k,o} \cdot r^{(o)}_{RB}$

2: Set $U^k_{i,t} = d^k_{i,t}$
3: For t from 1 to T, $\forall k,i$
4: If $h^k_{i,t} < h^{(min)}_{k,t}$, then $h^{(min)}_{k,t} = h^k_{i,t}$
5: If $U^k_{i,t} > U^{(max)}_{k,t}$, then $U^{(max)}_{k,t} = U^k_{i,t}$
   End

Table 2. Historical state recording function.

FUNCTION 3 Interference Mitigation
<Note>:This function addresses RB allocation according to UE conflict relationships

1: If $\chi_i(k, k') = 0$, $\forall k, k'$ and $Y_i(k, \tilde{k}) = 0$, $\forall k, \tilde{k}$
   Find any RB where $\sigma^{(n,y,t)}_{k,l,p} = 0$, $\sigma^{(n,y,t)}_{k',l,p} = 0$, and $\sigma^{(n,y,t)}_{\tilde{k},l,p} = 0$ to allocate, for UE k
2: Else if $Y_i(k, \tilde{k}) = 1$, find RB where $\sigma^{(n,y,t)}_{k',l,p} = 0$ and $\sigma^{(n,y,t)}_{k,l,p} = 0$ to allocate,
   but refrain RBs where $\sigma^{(n,y,t)}_{\tilde{k},l,p} = 1, \forall l,p$
3:   **Else if** $\chi_i(k, k') = 1$, find RB where $\sigma^{(n,y,t)}_{\tilde{k},l,p} = 0$ and $\sigma^{(n,y,t)}_{k,l,p} = 0$ to allocate,
      but refrain RBs where $\sigma^{(n,y,t)}_{k',l,p} = 1, \forall p$
   End

Table 3. Interference mitigation function.
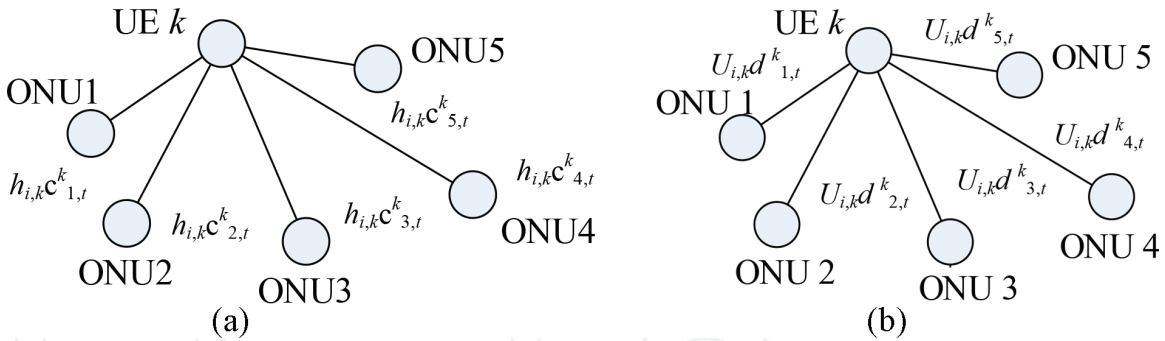
Figure 7. Wireless resource sharing logically on optical time/frequency blocks by different ONUs.

For each time slot t, the weight of each leaf is $h_{i,k}c^k_{i,t}$. The weight of edge between the rooted vertex and any leaf vertex i is $U_{i,k}d^k_{i,t}$, as shown in **Figure 7(b)**. Specifically, for $t = 1, 2,\ldots, T$, we define $h_{i,k} = min\{h^i_{k,t}, h^k_{j,t-1},\ldots, h^k_{j,1}\}$ and $U_{i,k} = min\{U^k_{k,t}, U^k_{j,t-1},\ldots, U^k_{j,1}\}$, respectively.

In the third step, the sharing path selection is performed by finding minimum delay time on each ONU. A sharing ONU combination could be found for UE k aiming to a minimum delay under its data rate demand.

In the fourth step, we allocate RB of CC to UEs in each ONU. Resource sharing for each UE (e.g., RB of CC) is executed by assigning $\sigma^{(n,y,t)}_{k,l,p}$. Here, $\sigma^{(n,y,t)}_{k,l,p}$ is a binary variable to define whether or not the n-th RB of the y-th CC on the l-th radio frame on p-th optical subcarrier is assigned to the k-th UE in slot t for finding a proper $c^k_{i,t}$ subjected to the minimum delay $d^k_{i,t}$ from a set of ONUs.

In the fifth step, the algorithm loops to another UE allocating RBs to it until all the UEs of current set have been finished. In the sixth step, the algorithm traverses all served ONUs to finish the RB allocation. In the seventh step, we compute the capacity obtained by UE k from ONU i in slot t and its delay time. Then we compare them to the previous historical values and update the historical peak value in the case that the current one exceeds it. After executing these steps, the algorithm outputs the RB set allocated to UE k classifying them into each subset of RBs obtained by each sharing ONU individually.

To meet all constrains of mathematical descriptions in Section 3, we formulate three different functions for the heuristic algorithm herein as practical approaches to achieve the target of optimization. Function 1 is one of solutions to search idle RBs for resource sharing satisfying minimum optical wavelength cost. Function 2 addresses historical information recording and their updating. Function 3 finds idle RBs and allocates them according to different UE conflict relationships in order to mitigate co-channel interference, which will be intensively evaluated and discussed in the next section of this chapter.

5. Simulations and numerical results

5.1. Simulation parameters

In this section, we provide a deep observation for the proposed resource sharing approach on the performance of wireless UEs in the OFDM-PON system. The simulation and analytic evaluation by large-scale C++ programming mainly focus on the interference mitigation of mobile UEs in the cell under different mobility and times.

In intensive large-scale C++ simulations, a RoF-OFDM-PON covering up to 256 cells assuming random UE mobility is deployed to evaluate our proposal as shown in **Figures 8** and **9**. Optical subcarriers with per λ_i 10-Gb/s digital-equivalent data rate are adopted. LTE-like wireless resources carried on optical subcarriers are assigned to UEs corresponding to the scheduling solution in the well-known network simulator 3 (ns-3) [17], supporting maximum five-carrier aggregation, simultaneously. MCS is assigned to UEs corresponding to Eqs. (12) and (13) by the scheduling in the ns-3. The main simulation parameters are described in **Table 4**.

In the C++ simulations, according to LTE-EPC model [18] in ns-3 simulator and with respect to its resource allocation models, we modify the scheduler significantly based on our proposed real-time sharing algorithm (RTSA). We evaluate the throughput performance of UEs by comparing RTSA with maximum throughput (MT) and proportional fair (PF) schemes [6, 19]. Note that for a fair comparison, we also modify the scheduler to serve multiple wavelength scheduling (i.e., multiple radio frames carried on one optical wavelength) since MT and PF themselves have no such functionality.

From the entire network perspective, the total UE number is set to 36,000 in simulations under different mobility ratios (a = number of mobile UEs/number of total UEs). We set a position for each UE with position allocator by model library of NS3 [17] (e.g., random waypoint). Mean-while, we aim to simulate a difference specifically on UE mobility, for example, changing the residential position of UEs (e.g., migrate and recall UEs) within the scope of all cells regularly
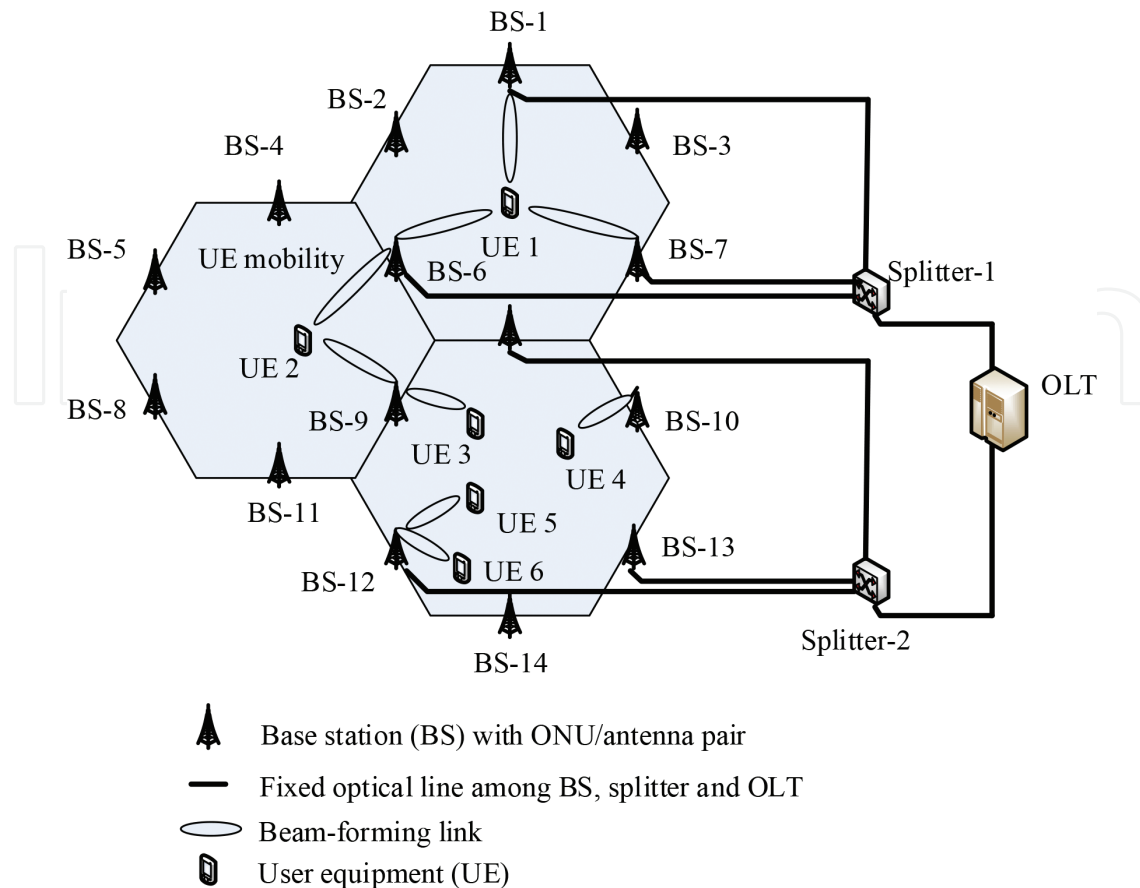
Figure 8. Scenarios of UEs and distributed antenna allocation in simulations with beamforming in the cluster of wireless cells.

in different times as shown in **Figure 9(a)** and **(b)** respectively. For instance, we define different mobility ratios of UEs equaling to 0.2 and 0.8, respectively.

5.2. Results and analysis on interference mitigation

Next, we observe the effect on interference mitigation under different UE mobility rates within different time slots by generating massive number of same angle UEs (the conflict UEs) in each beam direction. As an example, in **Figure 10** we typically illustrate four windows of UE distribution states under random mobility in four different time slots, respectively. With the irregular movement of UEs, new UE conflict relationships will be generated randomly in terms of different antennas. For instance, in the time slot 1, UE k_4 and k_5 are located in different directions in terms of antenna 1. Simultaneously, UE k_1 and k_7 which have a conflict relationship with each other are located in the same direction for antenna 1. However, in the time slot 2, a new UE conflict relationship is generated between UE k_4 and k_5, while UE k_1 and k_7 are located in different directions, and their conflict relationship disappears. Similarly, in a continuous time scope (e.g., 10 minutes) containing many more time slots, we then observe our proposed scheme in the aspect of interference cancellation. We therefore evaluate the block error rate (BLER) of RTSA, PF, and MT under Gauss interference model in ns-3 model library so as to compare our proposed scheme with conventional schemes in terms of their effectiveness on interference mitigation. In simulations, BLER is observed under fair channel condition, for instance, the same level of signal power which is set by signal-to-noise ratio (SNR), and the
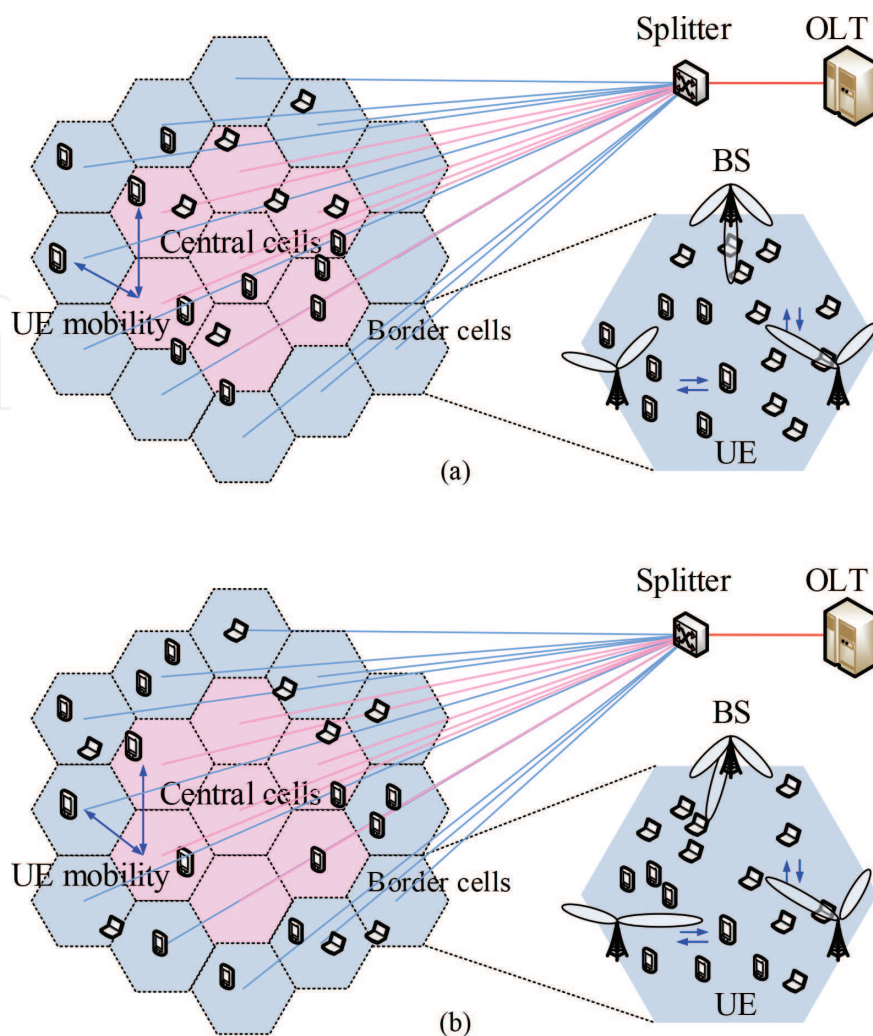
Figure 9. Scenarios of UE long-distance migration with position distribution for each UE by random model library (e.g., random waypoint) in simulations. (a) The aggregation of UEs at central cells. (b) The spreading of UEs to border cells.

Parameter	Value	Parameter	Value
LTE subcarrier	15 kHz	Frame duration	10 ms
Resource block	180 kHz	TTI	1 ms
RB carriers (N_{sub-c})	12	UE date rate$_{min}$ (R_k)	200 Mbps
RB OFDM symbols	7	MCS (J)	29
UE received CC$_{max}$ (z)	5	Bandwidth of CC	20 MHz
Single CC length (m)	100 RBs	Testing MIMO per cell	4×4
BS TX power	30 dBm	Number of cell	256
Noise spectral density	−174 dBm/Hz	Cell radius	500 m
Path loss (distance R), in dB	$128.1 + 37.6 \lg R$	SMF fiber distance	20 km

Table 4. Simulation parameters.

SNR is obtained according to the parameters in **Table 4**. In addition, we set random UE location and irregular mobility with the increase of time.

The change of BLER is observed under low mobility (a = 0.2) and high mobility (a = 0.8) cases, respectively. As shown in **Figure 11**, RTSA has the lowest level of BLER than MT and PF, which
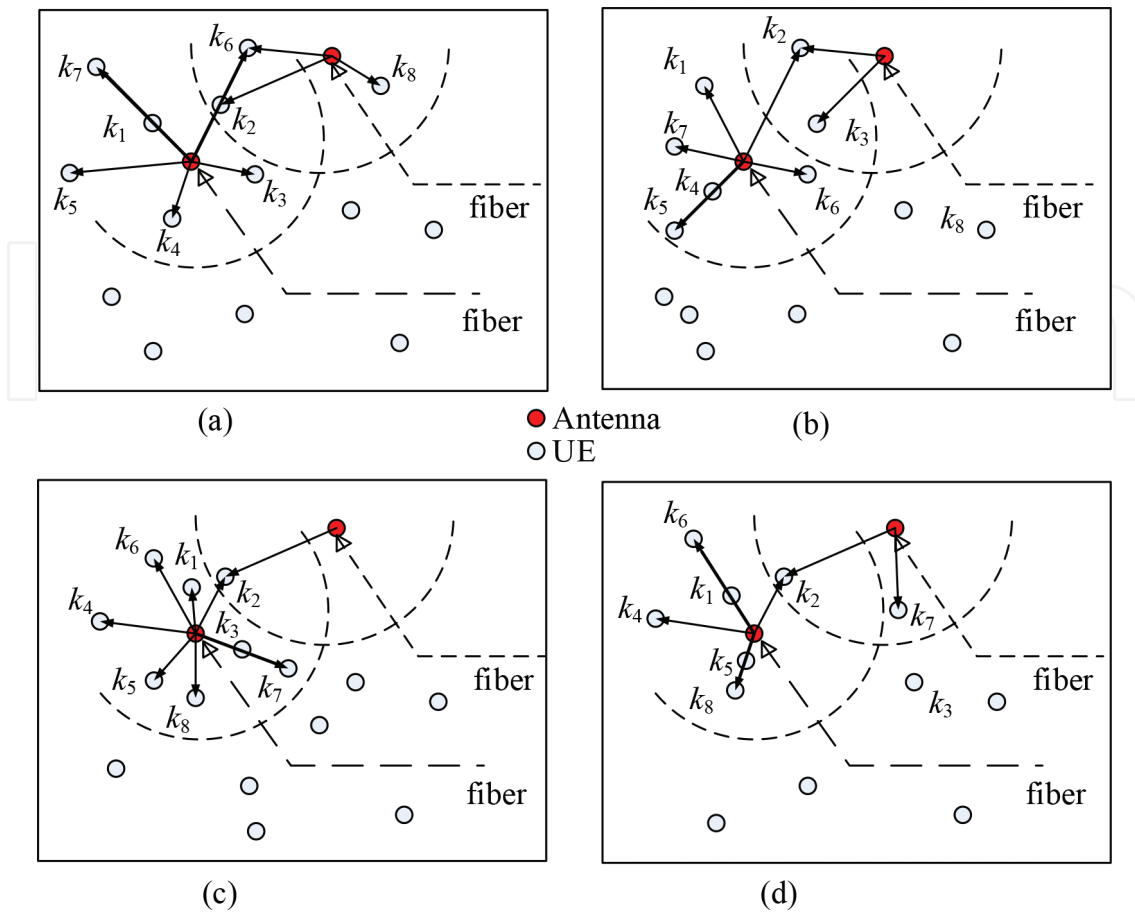
Figure 10. A group of observations about interference with UE/antenna distribution under different time slots and UE migration when employing the proposed scheme. In (a)–(d), the dashed line represents the propagation scope of each antenna. The solid arrow line represents a link with one beam direction (the thick arrow line represents a link which has conflict UEs with the potential interference).
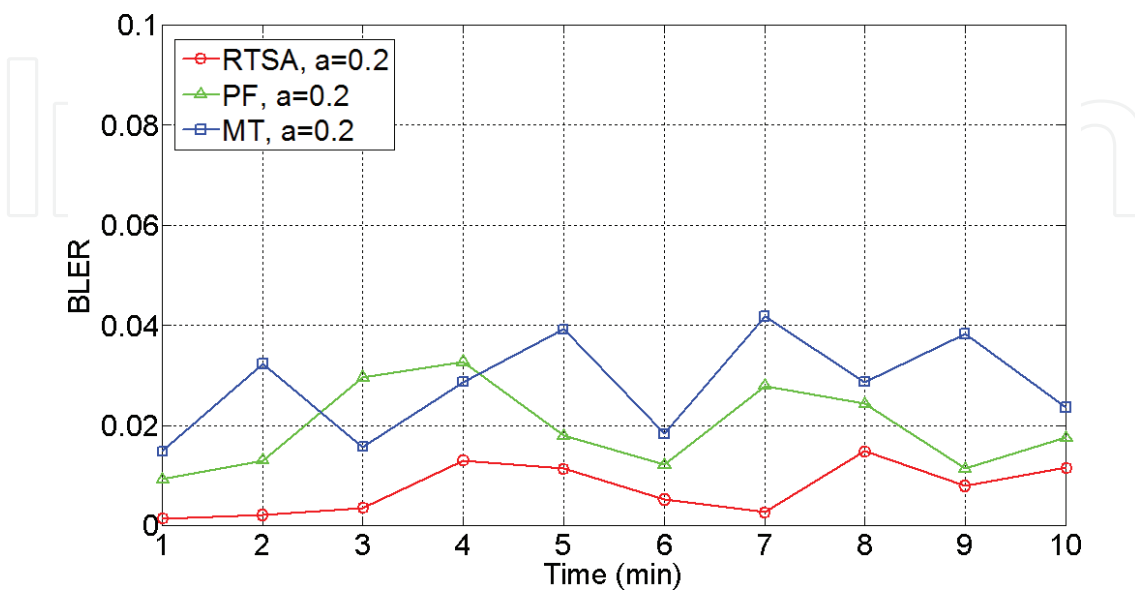

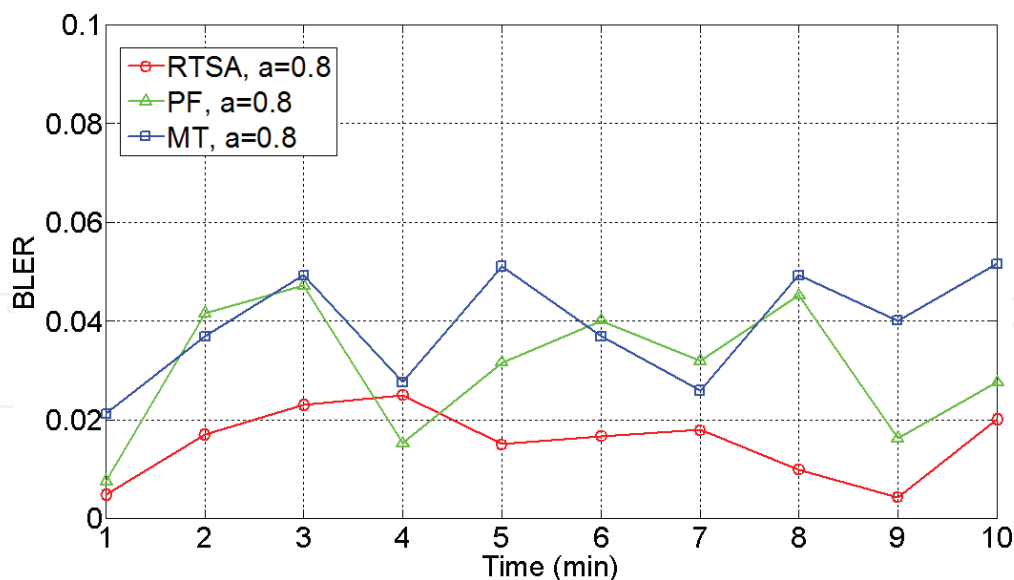**Figure 11.** Comparisons of BLER under different time durations (mobility ratio 0.2).

Figure 12. Comparisons of BLER under different time durations (mobility ratio 0.8).

also can be found in **Figure 12**. This feature reflects that the proposed RTSA has a benefit on BLER improvement. Compared with the results in **Figures 11** and **12**, we could further observe that the level of BLER for a = 0.8 is larger than that in a = 0.2 and the fluctuation of BLER in different time is also obvious in terms of the case where a = 0.2. The reason for a higher level of BLER is that a higher mobility brings much more interference with the conflict UEs generated in each beam direction. Nevertheless, our proposed RTSA will still has the lowest BLER level even in the case of higher UE mobility.

6. Conclusions

This chapter investigates the resource sharing problems for future 5G cellular networks [20], which jointly employ distributed massive MIMO, beamforming, and OFDMA-based passive optical network supporting radio-over-fiber (RoF). We have surveyed the system and its physical transmission features to explore reasonable solutions. With the assumptions based on physical features of system given in this chapter, we describe the latest hot problem with mathematical optimization for minimizing co-channel interference, etc. Since it is highly complex to get optimal results, then we heuristically formulate a real-time sharing algorithm as a practical solution. Simulation results also reveal that the proposed scheme is the most efficient one at the interference mitigation compared to conventional schemes.

Author details

Sheng Xu

Address all correspondence to: xusheng@akane.waseda.jp

Global Information and Telecommunication Institute, Waseda University, Tokyo, Japan

References

[1]   Bi S, Zhang R, Ding Z, Cui S. Wireless communications in the era of big data. *IEEE Communications Magazine*. 2015;**53**(10):190-199

[2]   Lin YM, Tien PL. Next-generation OFDMA-based passive optical network architecture supporting radio-over-fiber. *IEEE Journal on Selected Areas in Communications*. 2010;**28**(6): 791-799

[3]   Tien PL, Lin YM, Yuang MC. A novel OFDMA-PON architecture toward seamless broadband and wireless integration. In: *Conference on Optical Fiber Communication*; San Diego, CA, USA; 22-26 March 2009; IEEE; pp. 1, 3, 22-26

[4]   Zhang J, Wang T, Ansari N. An efficient MAC protocol for asynchronous ONUs in OFDMA PONs. In: *Optical Fiber Communication Conference and Exposition (OFC/NFOEC 2011) and The National Fiber Optic Engineers Conference*; Los Angeles, CA, USA; 6-10 March 2011; IEEE; pp. 1-3

[5]   Wei W, Hu J, Qian D, Ji PN, Wang T, Liu X, Qiao C. PONIARD: A programmable optical networking infrastructure for advanced research & development of future internet. *Journal of Lightwave Technology*. 18 February 2009;**27**(3):233-242

[6]   Wei W, Wang T, Qian D, Hu J. MAC protocols for optical orthogonal frequency division multiple access (OFDMA)-based passive optical networks. In: *Optical Fiber Communication/National Fiber Optic Engineers Conference (OFC/NFOEC 2008)*; San Diego, CA, USA; 24-28 February 2008; IEEE; pp. 1-3

[7]   You W, Yi L, Huang S, Chen J, Hu W. Power efficient dynamic bandwidth allocation algorithm in OFDMA-PONs. *IEEE/OSA Journal of Optical Communications and Networking*. 2013;**5**(12):1353-1360

[8]   Liu X, Effenberger F, Chand N, Zhou L, Lin H. Efficient mobile fronthaul transmission of multiple LTE-A signals with 36.86-Gb/s CPRI-equivalent data rate using a directly-modulated laser and fiber dispersion mitigation. In: *Asia Communications and Photonics Conference*; Shanghai, China; 11-14 November 2014; Optical Society of America (OSA); paper AF4B.5

[9]   Andrews JG, Buzzi S, Choi W, Hanly SV, Lozano A, Soong ACK, Zhang JC. What will 5G be? *IEEE Journal on Selected Areas in Communications*. 2014;**32**(6):1065-1085

[10] Almasoudi F, Alatawi K, Matin MA. Study of OFDM technique on RoF passive optical network. *Optics and Photonics Journal*. 2013;**3**:217-224

[11] Chow CW, Yeh CH, Wang CH, Wu CL, Chi S, Lin C. Studies of OFDM signal for broadband optical access networks. *IEEE Journal on Selected Areas in Communications*. 2010;**28**(6):800-807

[12] Kanonakis K, Tomkos I, Pfeiffer T, Prat J, Kourtessis P. ACCORDANCE: A novel OFDMA-PON paradigm for ultrahigh capacity converged wireline-wireless access networks. In: *12th International Conference on Transparent Optical Networks (ICTON2010)*; Munich, Germany; 27 June-1 July 2010; IEEE; pp. 1-4

[13] Qian D, Cvijetic N, Hu J, Wang T. 108 Gb/s OFDMAPON with polarization multiplexing and direct detection. *Journal of Lightwave Technology*. 2010;**28**(4):484-493

[14] Liao HS, Chen PY, Chen WT. An efficient downlink radio resource allocation with carrier aggregation in LTE-Advanced networks. *IEEE Transactions on Mobile Computing*. 2014;**13**(10): 2229-2239

[15] Cox C. An Introduction to LTE, LTE-Advanced, SAE, VoLTE and 4G Mobile Communications. West Sussex: Wiley; 2014

[16] Akyildiz IF, Gutierrez-Estevez DM, Reyes EC. The evolution to 4G cellular systems: LTE-advanced. *Physical Communication*. 2010;**3**:217-224

[17] NS-3 consortium. "NS-3 network simulator," http://www.nsnam.org/, INRIA and the University of Washington [Accessed September 2017]

[18] CTTC. "LTE-EPC network simulator (LENA)," CTTC, http://iptechwiki.cttc.es [Accessed October 2017]

[19] Guan N, Zhou Y, Tian L, Sun G, Shi J. Qos guaranteed resource block allocation algorithm for LTE systems. In: *IEEE 7th International Conference on Wireless and Mobile Computing, Networking and Communications (WiMob 2011)*; Wuhan, China; 10-12 October 2011; IEEE; pp. 307-312

[20] Xu S, Xu SG, Tanaka Y. Sub-carrier sharing in OFDM-PON for 5G mobile networks supporting radio-over-fibre. In: *21st OptoElectronics and Communications Conference (OECC 2016) held jointly with International Conference on Photonics in Switching (PS)*; Niigata, Japan; 3-7 July 2016; IEEE; pp. 1-3